

Cisplatin-conjugated gold nanoparticles as a theranostic agent for head and neck cancer

Erez Shmuel Davidi, MD¹ | Tamar Dreifuss, BSc²  | Menachem Motiei, PhD² |
Eliezer Shai, MSc³ | Dimitri Bragilovski, MSc⁴ | Leon Lubimov, BSc⁴ |
Marc Jose Jonathan Kindler, MSc⁴ | Aron Popovtzer, MD^{4,5} | Jeremy Don, PhD³ |
Rachela Popovtzer, PhD²

¹Department of Otolaryngology Head and Neck Surgery, Kaplan Medical Center, Rehovot, Israel

²Faculty of Engineering and the Institutes of Nanotechnology and Advanced Materials, Bar-Ilan University, Ramat-Gan, Israel

³The Mina and Everard Goodman Faculty of Life Sciences, Bar-Ilan University, Ramat-Gan, Israel

⁴Head and Neck Cancer Radiation Clinic, Institute of Oncology, Davidoff Cancer Center, Rabin Medical Center, Petah Tiqwa, Israel

⁵Sackler Faculty of Medicine, Tel-Aviv University, Ramat Aviv, Israel

Correspondence

Rachela Popovtzer, Faculty of Engineering and the Institutes of Nanotechnology and Advanced Materials, Bar-Ilan University, Ramat Gan 52900, Israel.

Email: rachela.popovtzer@biu.ac.il

Funding information

This work was partially supported by the Israel Cancer Research Fund (ICRF) and by the doctoral scholarship for applicable and scientific engineering research, granted to Tamar Dreifuss by the Ministry of Science and Technology, Israel.

Abstract

Background: The purpose of this study was to develop a nanoplatform, which simultaneously acts as radiosensitizer, drug carrier, and tumor imaging agent for head and neck cancer.

Methods: We synthesized 20 nm gold nanoparticles, coated with glucose and cisplatin (CG-GNPs). Their penetration into tumor cells and their cellular toxicity were evaluated in vitro. In vivo experiments were conducted to evaluate their impact on tumor growth and their imaging capabilities.

Results: The CG-GNPs showed efficient penetration into tumor cells and similar cellular toxicity as cisplatin alone. Combined with radiation, CG-GNPs led to greater tumor reduction than that of radiation alone and radiation with free cisplatin. The CG-GNPs also demonstrated efficient tumor imaging capabilities.

Conclusion: Our CG-GNPs have a great potential to increase antitumor effect, overcome resistance to chemotherapeutics and radiation, and allow imaging-guided therapy.

KEYWORDS

cancer, cisplatin, CT, gold nanoparticles, radiotherapy

1 | INTRODUCTION

Radiotherapy (RT) is a widely used strategy in cancer treatment, including head and neck squamous cell carcinoma (HNSCC). In advanced-stage tumors, RT is often combined

with chemotherapy (chemoradiotherapy) in order to improve the outcomes, and to avoid surgery and loss of patients' functions.^{1,2} This multitherapy strategy has led to significant improvement in the treatment paradigm of head and neck cancer. However, despite aggressive treatment, resistance of tumors remains a significant problem, leading to poor outcomes and negative prognoses.^{3,4} In addition, the

Erez Shmuel Davidi and Tamar Dreifuss contributed equally to this work.

chemotherapeutic drugs lead to severe side effects due to nonselective damaging of healthy cells.

The major chemotherapeutic drug for HNSCC is cisplatin (cis-Pt) and other platinum derivatives. The success of cisplatin in cancer treatment is derived from its ability to crosslink DNA and alter the structure.⁵ In addition, cisplatin activates various signal transduction pathways and, thus, induces apoptosis.⁶ However, cisplatin has a narrow therapeutic range, associated with significant systemic toxicity, which includes mainly nephrotoxicity, neurotoxicity, and ototoxicity. Over the years, different methods have been investigated, trying to avoid systemic exposure by specifically targeting the cancer cells, and, consequently, lower the diverse side effects.^{7,8}

Recently, nanoparticle-based approaches have been widely investigated for improving cancer therapy for both RT and chemotherapy strategies.⁹ Nanoagents containing high-Z materials (eg, Au, Gd, Bi, Hf, and W) have been used as radiosensitizers in many studies.^{4,10–13} High-Z materials increase radiation sensitivity due to their high X-ray absorption and emitting of secondary energy in the form of photoelectrons, auger electrons, and X-rays into surrounding tissue. Thus, high irradiation energy is concentrated inside the tumor, enhancing RT efficacy and specificity. Likewise, in order to reduce the systemic toxicity of chemotherapeutic drugs, many nanoparticle-based platforms have been utilized to specifically deliver drugs to the tumor by implementing both passive and active targeting approaches.^{14–16} Development of a single nanoparticle formulation that combines both radiosensitization and targeted drug delivery abilities, can significantly improve the therapeutic effect and treatment outcomes, as demonstrated in recent studies.^{3,17}

In the present work, we demonstrate a single nanopatform, consists of gold nanoparticles (GNPs) coated by cis-Pt and glucose (CG-GNPs), which simultaneously acts as a radiosensitizer and as a carrier that specifically delivers cisplatin to the A431 HNSCC tumor, leading to remarkable synergistic therapeutic effect. Due to the high atomic number of gold ($Z = 79$), and its well-known biosafety,^{4,18–20} GNPs are ideal candidates to be used as radiosensitizing agents. In addition, their unique physical, chemical, and biological properties, as well as the ability to attach multiple types of ligands to their surfaces, make them an excellent platform for targeted drug delivery. Although cisplatin conjugated GNPs have been previously investigated as RT enhancers using an *in vitro* model system of glioblastoma cells,²¹ this study is the first to evaluate this possibility *in vivo*, in a head and neck cancer model. In a previous study,²² we showed that glucose functionalized-GNPs (GF-GNPs) exhibit high accumulation in head and neck tumors, due to specific interaction with glucose transporter-1, which is overexpressed on the A431 cell membrane. Therefore, in addition to cisplatin, we coated our GNPs with glucose to increase the tumor

uptake rate. Our CG-GNPs showed, *in vitro* and *in vivo*, efficient penetration into tumor cells, and similar toxic effect as cisplatin alone at the same dose of cisplatin. Moreover, in combination with radiation treatment, CG-GNPs led to greater tumor reduction than that of the traditional chemoradiotherapy, which combines free cisplatin and RT treatment. Finally, as GNPs possess inherent CT imaging functions,^{23–30} our CG-GNPs demonstrated efficient tumor imaging capabilities. Therefore, this single nanoparticle formulation, which leads to better response to RT and allows tumor imaging, is a promising theranostic agent that has the potential to increase the anti-tumor effect, overcome resistance to chemotherapeutic agents and radiation, and allow imaging-guided therapy, enabling better therapeutic planning.

2 | MATERIALS AND METHODS

2.1 | Gold nanoparticle synthesis and conjugation with cisplatin and glucose

The gold nanoparticles (GNPs) were prepared using sodium citrate according to the known methodology described by Enustun and Turkevich.³¹ 0.414 mL of 1.4M HAuCl₄ solution (Strem Chemicals, Newburyport, MA) were added to 200 mL purified water in a 250 mL single-neck round bottom flask. The solution was heated in an oil bath on a hot plate until boiling. Then, 4.04 mL of a 10% sodium citrate solution (0.39M sodium citrate tribasic dihydrate 98%; Sigma-Aldrich, Rehovot, Israel) were then quickly added. The solution was stirred for 10 minutes, and then the flask was removed from the hot oil and placed aside until cooled. For the conjugation, first, the GNP solution was centrifuged to dispose of excess citrate. Then, in order to prevent aggregation and stabilize the particles in physiological conditions, O-(2-carboxyethyl)-O'-(2-mercaptoethyl) heptaethylene glycol (PEG7 95%; Sigma-Aldrich) solution was added to the GNPs, followed by stirring overnight and centrifugation in order to dispose of excess PEG7. The PEG7 layer also provides the chemical group required for antibody covalent binding (-COOH). The cisplatin and glucose conjugation was performed by adding excess amounts of N-ethyl-N-(3-dimethylaminopropyl) carbodiimide and N-hydroxysuccinimide (Thermo Fisher Scientific, Rockford, IL), followed by addition of 100 μ L, 25 mg/mL D-(+)-glucosamine hydrochloride (Sigma-Aldrich) and 150 μ L, 6 mg/mL cisplatin Cl₂-Pt-(NH₃)₂ (Sigma-Aldrich). For GF-GNP synthesis, the same procedure has been done, without the cisplatin addition. Finally, GNPs were centrifuged until final Au concentration of 30 mg/mL, as measured by atomic absorption spectroscopy. According to inductively coupled plasma analysis of cisplatin concentration, this GNP solution contained 1.13 mg/mL cisplatin. Schematic diagram of the synthesis is presented in Figure 1.

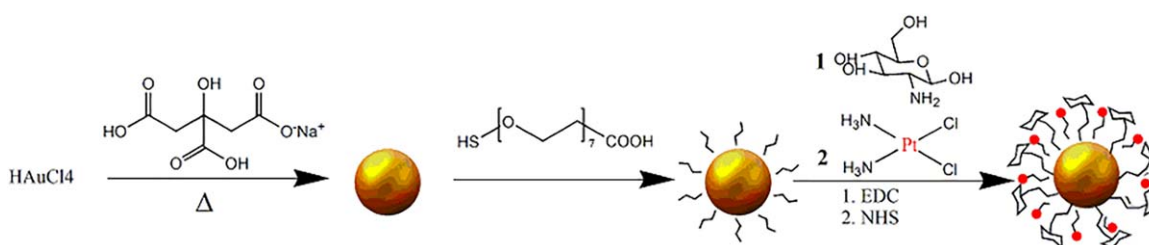


FIGURE 1 Schematic diagram of the synthesis of cisplatin and glucose-coated gold nanoparticles (CG-GNPs). EDC, N-ethyl-N-(3-dimethylamino-propyl) carbodiimide; NHS, N-hydroxysuccinimide [Color figure can be viewed at wileyonlinelibrary.com]

2.2 | In vitro cell binding experiment

The A431 cells (0.7×10^6) were seeded in 60-mm dishes with 5 mL Dulbecco's modified Eagle's medium containing 5% fetal calf serum, 0.5% penicillin, and 0.5% glutamine. Cells were incubated for 30 minutes at 37°C, with CG-GNPs and GF-GNPs ($n = 3$ per group). After incubation, the medium was removed and cells were washed twice with phosphate buffered saline (PBS). Then, cells were collected and gold concentrations in the samples were measured using flame atomic absorption spectroscopy.

2.3 | In vitro cell survival and DNA damage experiments

The quantitative in vitro study consisted of 4 groups ($n = 3$ per group): (1) A431 cells with CG-GNPs; (2) A431 cells with GF-GNPs; (3) A431 cells with free cisplatin; and (4) A431 cells without GNPs or cisplatin. The A431 cells (1×10^6) in 5-mL Dulbecco's modified Eagle's medium containing 5% fetal calf serum, 0.5% penicillin and 0.5% glutamine, were seeded in 60 mm dishes and incubated at 37°C for 48 hours with or without the different complexes. The GNPs were added in total amount of 10 μ L (approximately 11 μ g cisplatin). The cisplatin was added in equivalent dose. After 48 hours of incubation, the medium was washed twice with PBS and the remaining cells were taken for cell counting on counting chambers in order to compare the number of cells between the different groups. For evaluation of DNA damage, cells were seeded on glass cover slips in 35-mm dishes. After 24 hours of incubation at 37°C, the cells were incubated with the various complexes for 1 hour. Then, the cells were washed twice with PBS followed by fixation with 4% paraformaldehyde for 45 minutes at room temperature and washing with PBS. The irradiated cells were irradiated before fixation using a Varian linear accelerator (Davidoff Cancer Center) at a 6 MV energy, 25 Gy.

2.4 | Immunocytochemistry

Fixed cells were permeabilized and blocked with 0.5% Triton X-100 (Sigma-Aldrich, Rehovot, Israel) in fetal bovine serum for 1 hour. Next, the cells were treated with phospho-histone H2A.X (Ser139) rabbit monoclonal antibody (Cell Signaling,

Rehovot, Israel) at 1:400 dilution overnight at 4°C. The cells were then washed with PBS and stained with Alexa Fluor 594 secondary antibody (Thermo Fisher Scientific) at 1:400 dilution for 1 hour at room temperature. After washing with PBS, the nuclei were stained with diamidino-phenylindole in fluorescent mounting medium (GBI Laboratories, Mukilteo, WA) and glass cover slips were mounted on the microscope slides. The slides were imaged on a ZEISS AxioImager Z1 microscope. Fluorescence detection was performed using laser excitation with the appropriate dichroics and emission filters for the diamidino-phenylindole and Alexa 594 dyes.

2.5 | Animal model and in vivo experiments

The in vivo study was conducted in compliance with the protocols approved by the Animal Care and Use Committees of Bar Ilan University, Ramat Gan, Israel. The A431 cells (2×10^6) were injected s.c. into the back flank area of nude mice aged 6 weeks. When the tumor size reached a diameter of 4–5 mm, 200 μ L of CG-GNPs (0.22 mg cisplatin) or equivalent dose of free cisplatin were i.v. injected into their tail vein (in accordance to the clinical dosage used for HNSCC treatment, which is about 10 mg/kg). For the biodistribution study, CG-GNPs were injected into 3 mice. Twenty-four hours postinjection, the mice were euthanized and gold concentrations in the tumor and major organs (liver, spleen, brain, kidneys, and blood) were quantitatively measured by flame atomic absorption spectroscopy. Tumor toxicity of CG-GNPs, in comparison to free cisplatin, was investigated with and without combination of RT. Mice were divided into 6 groups ($n = 3$ per group): (1) no treatment; (2) treatment with free cisplatin; (3) treatment with CG-GNPs; (4) X-ray irradiation alone (RT); (5) RT + free cisplatin; and (6) RT + CG-GNP (see Table 1). Irradiated mice were irradiated the same day using a Varian linear accelerator (Davidoff Cancer Center) at a 6 MV dosage, which is the standard clinical radiation energy used in head and neck cancers. Tumor growth was measured using a caliper in various time points, until 24 days postinjection. Then, the mice were euthanized. To evaluate the imaging capabilities of CG-GNPs, 3 mice that had been injected with CG-GNPs were scanned by micro-CT scanner (Skyscan High Resolution Model 1176) before injection, 30 minutes postinjection, and 7 days postinjection.

TABLE 1 Summary of the experimental groups (in vivo experiment)

Group number	Type of treatment
Group 1	Control (no treatment)
Group 2	Free cisplatin
Group 3	CG-GNPs
Group 4	RT
Group 5	RT + free cisplatin
Group 6	RT + CG-GNPs

Abbreviations: CG-GNPs, cisplatin and glucose-coated gold nanoparticles; RT, radiotherapy.

2.6 | Atomic absorption spectroscopy analysis

Flame atomic absorption spectroscopy (spectrAA 140; Agilent Technologies) was used to determine gold concentrations in the investigated samples. Cell samples from the in vitro experiments were dissolved in 100 μ L aqua regia acid (nitric acid and hydrochloric acid, volume ratio 1:3) and diluted with purified water to a total volume of 4 mL. For the in vivo experiment, tissues were melted in 1 mL aqua regia acid and then evaporated and diluted to a total volume of 10 mL. After filtration of the samples, gold concentrations were determined according to absorbance values, with correlation to calibration curves.

2.7 | CT analysis

The CT scans were performed using a micro-CT scanner (Skyscan High Resolution Model 1176) with nominal resolution of 35 μ m, 0.2 mm aluminum filter, and tube voltage of 45 kV. Reconstruction was done with a modified Feldkamp³² algorithm using the SkyScanNRecon software accelerated by GPU.³³ Ring artifact reduction, Gaussian smoothing (3%), and beam hardening correction (20%) were applied. Three-dimensional (3D) images were generated using SkyScan CT-Voxel (“CTVox”) software.

3 | RESULTS AND DISCUSSION

3.1 | Gold nanoparticle synthesis and characterization

20 nm GNPs were successfully synthesized and coated first with PEG7, and then with cisplatin and glucose for CG-GNPs, or glucose only for GF-GNPs as control particles. The 20 nm GNPs were chosen due to their efficient uptake in tumor cells,^{34,35} and their low toxicity profile.⁴ The PEG

coating serves to reduce particle opsonization and recognition by the reticuloendothelial system in the spleen and, thus, it prolongs the blood circulation of the particle.^{36,37} Glucose was conjugated to the GNPs through its second carbon atom, in order to enhance GNP uptake by cancer cells. In our previous work,²² we had showed, both in vitro and in vivo, that this type of conjugation, compared to conjugation through other carbon residues, allows the GNPs to better enter into A431 cancer cells in a process of receptor mediated endocytosis. Characterization of GNPs was carried out using transmission electron microscopy, UV-Vis spectroscopy, and zeta potential measurements (see Figure 2). The transmission electron microscopy image shows uniform, spherical GNPs, with a mean size of about 20 nm in diameter. The different coating layers were confirmed by UV-Vis plasmon resonance shift and expansion and by zeta potential measurements. In addition, as measured by inductively coupled plasma-mass spectrometry, the GNP solution (with Au concentration of 30 mg/mL) contained 1.13 mg/mL cisplatin.

3.2 | In vitro experiments

First, to evaluate CG-GNP ability to penetrate into A431 cells, CG-GNPs were incubated with A431 cells for 30 minutes at 37°C. The observed uptake, as measured by flame atomic absorption spectroscopy, was compared to that of GF-GNPs, which have been proven before to be highly preferred by cancer cells.²² As shown in Figure 3A, non-significant difference in uptake rate was observed for GF-GNP and CG-GNP, probably due to the glucose that is also attached to the GNP. Next, in order to assess the toxic effect of CG-GNPs on A431 cells, we measured cell survival after 48 hours of incubation with CG-GNPs, in comparison to that of control cells without GNPs, and to that of cells after incubation with equivalent amounts of free cisplatin, or with GF-GNPs, to confirm that the toxic effect was due to the cisplatin coating and not due to the GNP itself. The results are shown in Figure 3B. By comparing 3 different exposure groups to the control population of A431 cells, it was clearly shown that both free cisplatin and CG-GNPs had reached a same significant ($P < .01$) toxic reaction compared with the control groups, suggesting that the cisplatin preserves its toxic activity while conjugated to the GNP. Therefore, CG-GNPs can be used as an efficient drug carrier.

Because one of the earliest events detected in cells after exposure to DNA damaging agents and RT is immediate formation of γ -H2AX,³⁸ we assessed its formation in vitro after treatment with the various complexes, with or without irradiation, by immunocytochemistry. As demonstrated in Figure 4, the intensity of γ -H2AX staining (red) in the radiated cells was clearly higher than that of the nonradiated cells. Among the radiated cells, the highest intensity was observed for the cells

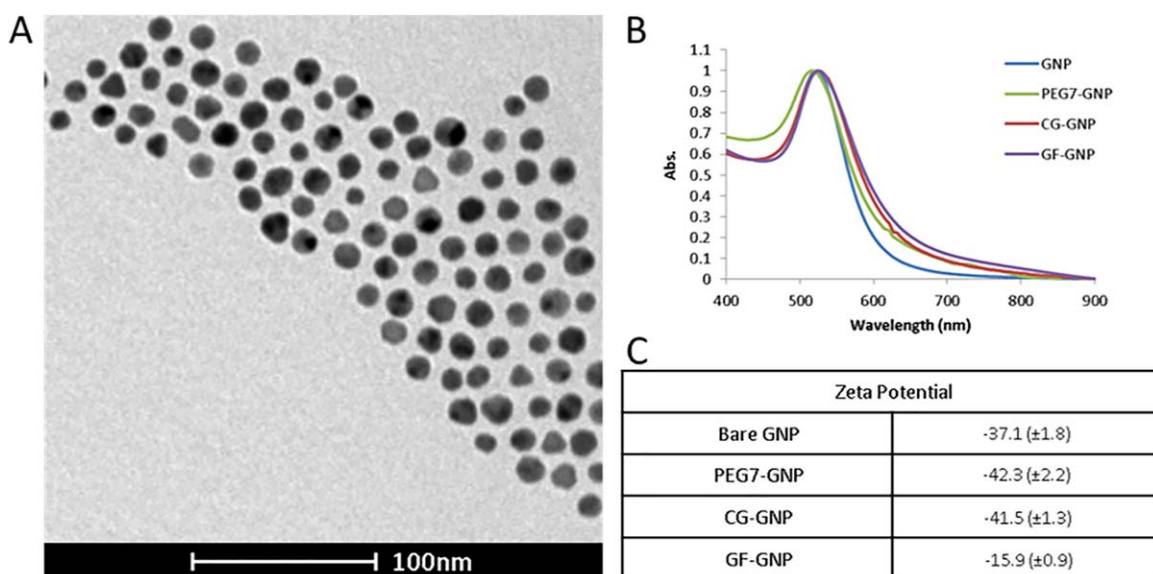


FIGURE 2 Characterization of gold nanoparticles (GNPs). A, Transmission electron microscopy image of approximately 20 nm spherical GNPs. B, UV-vis spectroscopy of bare GNPs, PEG7-GNPs, cisplatin and glucose (CG)-GNPs, and glucose functionalized (GF)-GNPs. C, Zeta potential measurements [Color figure can be viewed at wileyonlinelibrary.com]

that were preincubated with CG-GNPs. In addition, it can be seen that cells that were incubated with free cisplatin or CG-GNPs without follow-up irradiation exhibited some degree of DNA break, in contrast to the GF-GNPs, which showed no toxic effect on the cells. These results demonstrate that the increased toxic activity of CG-GNPs, alone and in combination with radiation arises from increasing DNA damage.

3.3 | In vivo evaluation of cisplatin-conjugated gold nanoparticle ability to enhance radiotherapy

In order to investigate in vivo the possibility of CG-GNP to enhance RT, mice bearing A431 tumors were randomly

divided into 6 groups ($n = 3$ per group): (1) no treatment; (2) treatment with free cisplatin; (3) treatment with CG-GNPs; (4) X-ray irradiation alone (RT); (5) RT + free cisplatin; and (6) RT + CG-GNP. Radiated mice were irradiated 6 hours postinjection with a 6 MV dosage, which is the standard clinical radiation energy used in head and neck cancers. Tumor size was measured in various time points, until 24 days postinjection (see Figure 5). Among the nonirradiated mice, no difference was observed between the groups, which all exhibited high tumor growth. In contrast, all irradiated mice showed some degree of tumor growth inhibition. Given that the external beam RT is considered as a major strategy in treating localized aggressive head and neck cancers, the nonsignificant antitumor effect of free

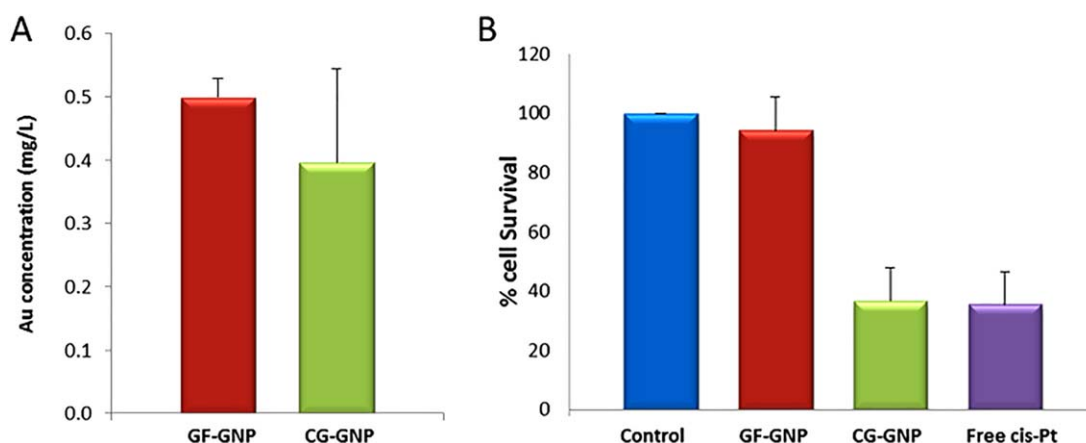


FIGURE 3 A, Gold concentration in A431 cells after 30 minutes of incubation with glucose functionalized-gold nanoparticles (GF-GNPs) or cisplatin and glucose (CG)-GNPs, as measured by flame atomic absorption spectroscopy. B, Cell survival after 48 hours of incubation with CG-GNPs, GF-GNPs, or free cisplatin. The CG-GNPs cause a significant toxic reaction, similar to cisplatin alone. One hundred percent was defined as the number of cells in the control group after 48 hours of incubation. Results are presented as mean \pm SD. cis-Pt, cisplatin [Color figure can be viewed at wileyonlinelibrary.com]

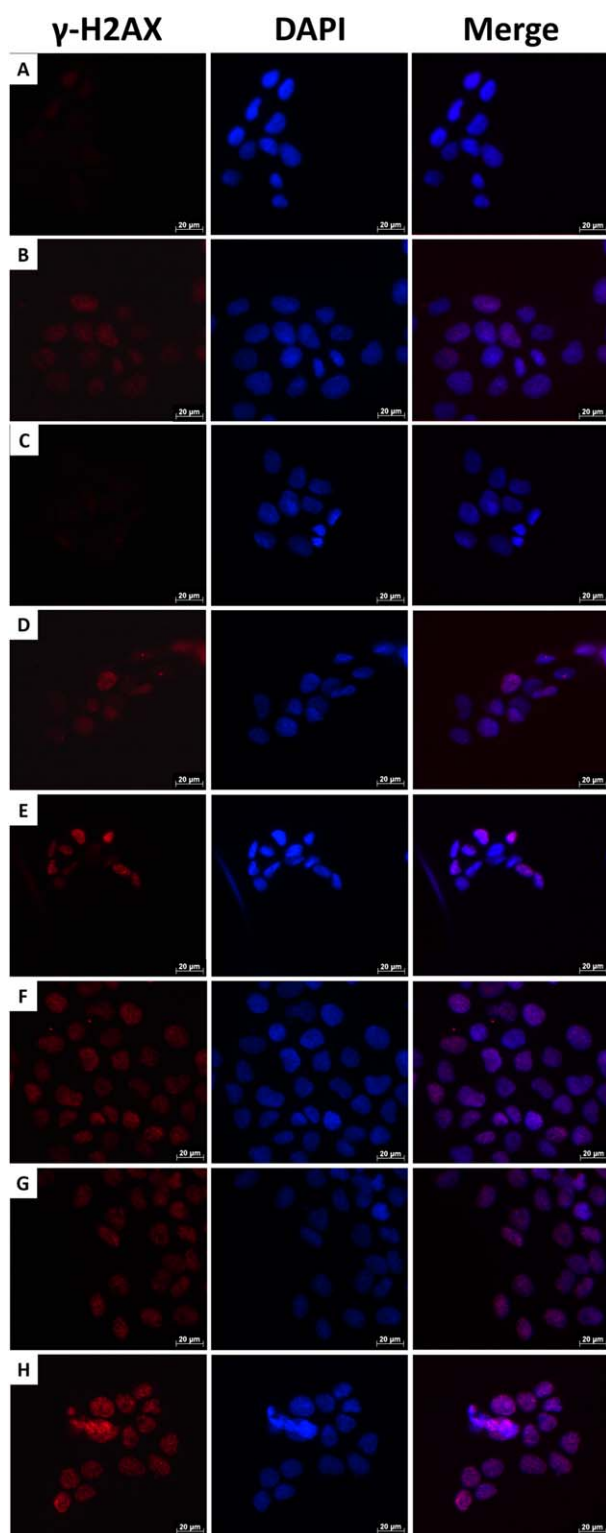


FIGURE 4 Representative immunocytochemistry of γ -H2AX in A431 cells after various treatments. A, No treatment; B, free cisplatin; C, glucose functionalized (GF)-gold nanoparticles (GNPs); D, cisplatin and glucose (CG)-GNPs; E, X-ray irradiation (radiotherapy [RT]); F, RT + free cisplatin; G, RT + GF-GNPs; H, RT + CG-GNPs. Strong induction of γ -H2AX foci was detected in the irradiated cells, whereas the highest intensity was observed for the cells that were preincubated with CG-GNPs. Scale bar: 20 μ m. cis-Pt, cisplatin [Color figure can be viewed at wileyonlinelibrary.com]

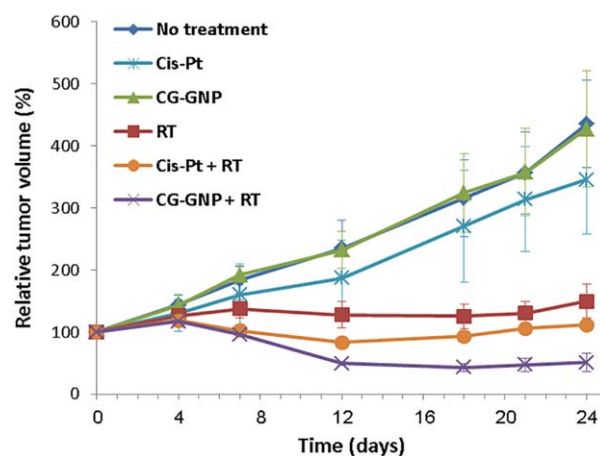


FIGURE 5 Tumor growth rate in 6 groups of mice: (1) no treatment; (2) treatment with free cisplatin; (3) treatment with cisplatin and glucose-gold nanoparticles (CG-GNPs); (4) X-ray irradiation alone (radiotherapy [RT]); (5) RT + free cisplatin; and (6) RT + CG-GNP. Significant reduction in tumor volume was observed in mice treated with CG-GNP + RT. Results are presented as mean \pm SEM. cis-Pt, cisplatin [Color figure can be viewed at wileyonlinelibrary.com]

cisplatin and CG-GNPs without the addition of external RT is not surprising. Interestingly, among the irradiated mice, CG-GNPs offered a definite shrinkage of tumor, better than that of radiation alone, and, furthermore, better than that of the traditional chemoradiotherapy, which combines free cisplatin and radiation. This is due to the inherent characteristic of GNPs that serve as radiosensitizers, together with their ability to specifically deliver cisplatin to the tumor site. Tumor size in this group (CG-GNPs) remained stable until day 7 and then shrunk to about 50% of the initial size until day 24. The final sizes of tumors in the other groups of irradiated mice were 150% and 110% for RT alone and RT + cisplatin, respectively (see Figure 5). In addition, in a prior study with HNSCC,⁴ we have shown the antitumor effect of radiation treatment in combination with immunoglobulin G-coated GNPs, which was significantly lower than that of RT + CG-GNP, as obtained in this study. The CG-GNPs

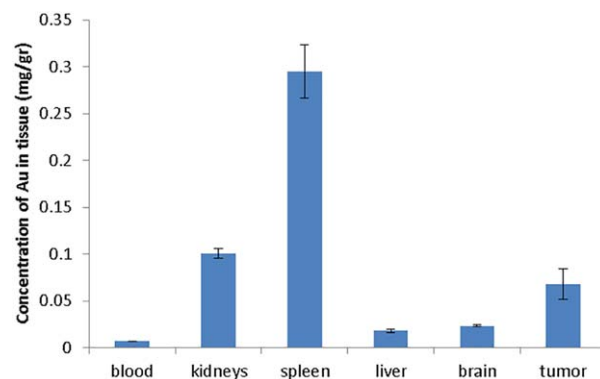


FIGURE 6 Biodistribution of cisplatin and glucose-gold nanoparticles (CG-GNPs) in the main organs at 24 hours postinjection. Results presented as mean \pm SEM [Color figure can be viewed at wileyonlinelibrary.com]

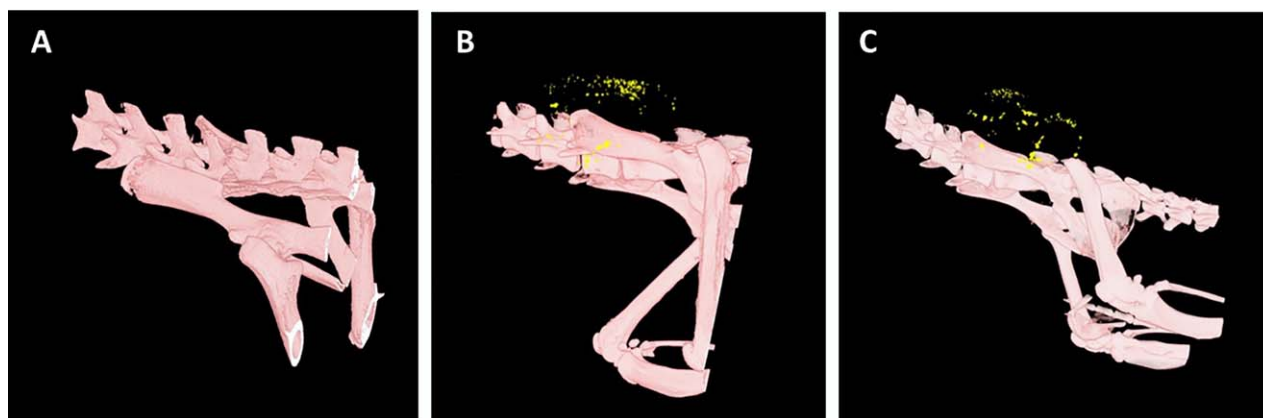


FIGURE 7 CT images of a representative mouse (tumor region) at several time points: A, before cisplatin and glucose-gold nanoparticle injection; B, 30 minutes postinjection; and C, 7 days postinjection [Color figure can be viewed at wileyonlinelibrary.com]

not only slowed the rate of tumor growth as immunoglobulin G-coated GNPs (which can act as radiosensitizers solely), but also significantly reduced the tumor. These results highlight the significant synergistic effect of our chemoradiotherapy agent, which may also benefit to reduce cisplatin systemic toxicity.

3.4 | In vivo biodistribution studies

In order to investigate the whole-body distribution of CG-GNPs, CG-GNPs were i.v. injected into 3 mice bearing A431 tumors. At 24 hours postinjection, mice were euthanized and gold concentrations in the tumor and major organs (liver, spleen, brain, kidneys, and blood) were quantitatively measured by flame atomic absorption spectroscopy (see Figure 6). As expected, a relatively high amount of gold was observed in the tumor. Additionally, the results indicate that CG-GNPs are cleared mainly by the reticuloendothelial system, as suspected. The spleen has a much larger role than the liver at 24 hours postinjection and a significant amount of gold has been observed also in the kidneys. Interestingly, there seems to be a small amount of GNPs in the brain, suggesting that part of the particles managed to cross the blood brain barrier, probably because of the glucose coating. It is important to note that the amount of gold in the cerebral blood was deducted from the total amount of gold found in the brain to exclude gold that did not cross the blood brain barrier. The amount of gold in the cerebral blood was calculated by measuring the concentration of gold in the blood and multiplying by the cerebral blood weight, which is about 5.8% of the weight of the brain.³⁹ The biodistribution data matches other publications, dealing with 20 nm GNPs.^{40,41}

3.5 | In vivo CT experiments

Next, the ability of CT to detect tumors as a result of CG-GNP accumulation at the tumor site was evaluated. The mice were

scanned by micro-CT scanner before injection, 30 minutes postinjection, and 7 days postinjection. As can be seen in Figure 7, CG-GNPs rapidly accumulated within tumor tissue, whereas after 7 days there were still significant amounts of gold in the tumor. Therefore, a single injection of CG-GNP will enable the prolonged therapeutic effect of cisplatin as well as possibility of long-term imaging and follow-up.

4 | CONCLUSIONS

To summarize, in this study, we presented a single nanoplat-form, consisting of gold nanoparticles coated with cisplatin and glucose, which simultaneously acts as a radiosensitizer, as a carrier that specifically delivers cisplatin to the tumor, and as an efficient CT contrast agent. Using an HNSCC model, we first showed in vitro that our nano-formulation penetrates efficiently into tumor cells, and has the similar toxic effect as cisplatin alone at the same dose of cisplatin. Moreover, we demonstrated in vivo that in combination with RT, our CG-GNPs significantly enhance tumor growth inhibition in comparison to RT alone, and, moreover, in comparison to the combination of RT with free cisplatin. In addition, we demonstrated the feasibility of CG-GNP as a CT contrast agent. Therefore, this single nano-formulation has the potential to increase the antitumor effect, overcome resistance to chemotherapeutics and radiation, and allow tumor diagnosis by CT imaging and better therapeutic planning. Future studies will include multiple CG-GNP injections as well as multiple radiation sessions to resemble the current clinical approach with human patients.

ACKNOWLEDGMENTS

This work was partially supported by the Israel Cancer Research Fund (ICRF), by the Israel Science Foundation (ISF) and by the doctoral scholarship for applicable and scientific engineering research, granted to Tamar Dreifuss by the Ministry of Science and Technology, Israel.

FINANCIAL AND COMPETING INTEREST DISCLOSURE

The authors have declared that no competing interest exists. No writing assistance was utilized in the production of this manuscript.

ORCID

Tamar Dreifuss, BSc  <http://orcid.org/0000-0001-7399-9802>

REFERENCES

- [1] Wolf GT, Hong WK, Fisher SG, et al. Induction chemotherapy plus radiation compared with surgery plus radiation in patients with advanced laryngeal cancer. The Department of Veterans Affairs Laryngeal Cancer Study Group. *N Engl J Med*. 1991; 324:1685-1690.
- [2] Bernier J, Dommange C, Ozsahin M, et al. Postoperative irradiation with or without concomitant chemotherapy for locally advanced head and neck cancer. *N Engl J Med*. 2004;350:1945-1952.
- [3] Song G, Chao Y, Chen Y, et al. All-in-one theranostic nanoplat-form based on hollow TaOx for chelator-free labeling imaging, drug delivery, and synergistically enhanced radiotherapy. *Adv Funct Mater*. 2016;26:8243-8254.
- [4] Popovtzer A, Mizrahi A, Motiei M, et al. Actively targeted gold nanoparticles as novel radiosensitizer agents: an in vivo head and neck cancer model. *Nanoscale*. 2016;8:2678-2685.
- [5] Takahara PM, Rosenzweig AC, Frederick CA, Lippard SJ. Crystal structure of double-stranded DNA containing the major adduct of the anticancer drug cisplatin. *Nature*. 1995;377:649-652.
- [6] Florea AM, Büsselberg D. Cisplatin as an anti-tumor drug: cellular mechanisms of activity, drug resistance and induced side effects. *Cancers (Basel)*. 2011;3:1351-1371.
- [7] Dhar S, Gu FX, Langer R, Farokhzad OC, Lippard SJ. Targeted delivery of cisplatin to prostate cancer cells by aptamer functionalized Pt(IV) prodrug-PLGA-PEG nanoparticles. *Proc Natl Acad Sci U S A*. 2008;105:17356-17361.
- [8] Schechter B, Arnon R, Wilchek M. Polymers in drug delivery: immunotargeting of carrier-supported cis-platinum complexes. *React Polym*. 1995;25:167-175.
- [9] Kwatra D, Venugopal A, Anant S. Nanoparticles in radiation therapy: a summary of various approaches to enhance radiosensitization in cancer. *Transl Cancer Res*. 2013;2:330-342.
- [10] Song G, Chen Y, Liang C, et al. Catalase-loaded TaOx nano-shells as bio-nanoreactors combining high-z element and enzyme delivery for enhancing radiotherapy. *Adv Mater*. 2016;28:7143-7148.
- [11] Song G, Liang C, Yi X, et al. Perfluorocarbon-loaded hollow Bi₂Se₃ nanoparticles for timely supply of oxygen under near-infrared light to enhance the radiotherapy of cancer. *Adv Mater*. 2016;28:2716-2723.
- [12] Al Zaki A, Joh D, Cheng Z, et al. Gold-loaded polymeric micelles for computed tomography-guided radiation therapy treatment and radiosensitization. *ACS Nano*. 2014;8:104-112.
- [13] Joh DY, Kao GD, Murty S, et al. Theranostic gold nanoparticles modified for durable systemic circulation effectively and safely enhance the radiation therapy of human sarcoma cells and tumors. *Transl Oncol*. 2013;6:722-731.
- [14] Murphy EA, Majeti BK, Barnes LA, et al. Nanoparticle-mediated drug delivery to tumor vasculature suppresses metastasis. *Proc Natl Acad Sci U S A*. 2008;105:9343-9348.
- [15] Singh R, Lillard JW. Nanoparticle-based targeted drug delivery. *Exp Mol Pathol*. 2009;86:215-223.
- [16] Dreifuss T, Barnoy E, Motiei M, Popovtzer R. Theranostic gold nanoparticles for CT imaging. In: *Design and Applications of Nanoparticles in Biomedical Imaging*. Bulte JWM, Modo MMJ, eds. Cham, Switzerland: Springer International Publishing; 2017:403-427.
- [17] Park J, Park J, Ju EJ, et al. Multifunctional hollow gold nanoparticles designed for triple combination therapy and CT imaging. *J Control Release*. 2015;207:77-85.
- [18] Connor EE, Mwamuka J, Gole A, Murphy CJ, Wyatt MD. Gold nanoparticles are taken up by human cells but do not cause acute cytotoxicity. *Small*. 2005;1:325-327.
- [19] Villiers C, Freitas H, Couderc R, Villiers MB, Marche P. Analysis of the toxicity of gold nano particles on the immune system: effect on dendritic cell functions. *J Nanopart Res*. 2010;12:55-60.
- [20] Betzer O, Meir R, Dreifuss T, et al. In-vitro optimization of nanoparticle-cell labeling protocols for in-vivo cell tracking applications. *Sci Rep*. 2015;5:15400.
- [21] Setua S, Ouberei M, Piccirillo SG, Watts C, Welland M. Cisplatin-tethered gold nanospheres for multimodal chemoradiotherapy of glioblastoma. *Nanoscale*. 2014;6:10865-10873.
- [22] Motiei M, Dreifuss T, Betzer O, et al. Differentiating between cancer and inflammation: a metabolic-based method for functional computed tomography imaging. *ACS Nano*. 2016;10:3469-3477.
- [23] Lusic H, Grinstaff MW. X-ray-computed tomography contrast agents. *Chem Rev*. 2013;113:1641-1666.
- [24] Meir R, Motiei M, Popovtzer R. Gold nanoparticles for in vivo cell tracking. *Nanomedicine (Lond)*. 2014;9:2059-2069.
- [25] Shilo M, Sharon A, Baranes K, Motiei M, Lellouche JP, Popovtzer R. The effect of nanoparticle size on the probability to cross the blood-brain barrier: an in-vitro endothelial cell model. *J Nanobiotechnology*. 2015;13:19.
- [26] Arvizo R, Bhattacharya R, Mukherjee P. Gold nanoparticles: opportunities and challenges in nanomedicine. *Expert Opin Drug Deliv*. 2010;7:753-763.
- [27] Hainfeld JF, Slatkin DN, Focella TM, Smilowitz HM. Gold nanoparticles: a new x-ray contrast agent. *Br J Radiol*. 2006;79: 248-253.
- [28] Betzer O, Shwartz A, Motiei M, et al. Nanoparticle-based CT imaging technique for longitudinal and quantitative stem cell tracking within the brain: application in neuropsychiatric disorders. *ACS Nano*. 2014;8:9274-9285.
- [29] Meir R, Shamalov K, Betzer O, et al. Nanomedicine for cancer immunotherapy: tracking cancer-specific T-cells in vivo with gold nanoparticles and CT imaging. *ACS Nano*. 2015;9:6363-6372.
- [30] Rand D, Ortiz V, Liu Y, et al. Nanomaterials for x-ray imaging: gold nanoparticle enhancement of x-ray scatter imaging of hepatocellular carcinoma. *Nano Lett*. 2011;11:2678-2683.

- [31] Enustun BV, Turkevich J. Coagulation of colloidal gold. *J Am Chem Soc.* 1963;85:3317-3328.
- [32] Feldkamp LA, Davis LC, Kress JW. Practical cone-beam algorithm. *J Opt Soc Am A.* 1984;1:612-619.
- [33] Yan G, Tian J, Zhu S, Dai Y, Qin C. Fast cone-beam CT image reconstruction using GPU hardware. *J Xray Sci Technol.* 2008;16:225-234.
- [34] Dreifuss T, Betzer O, Shilo M, et al. A challenge for theranostics: is the optimal particle for therapy also optimal for diagnostics? *Nanoscale.* 2015;7:15175-15184.
- [35] Duncan B, Kim C, Rotello VM. Gold nanoparticle platforms as drug and biomacromolecule delivery systems. *J Control Release.* 2010;148:122-127.
- [36] Dancey JE, Chen HX. Strategies for optimizing combinations of molecularly targeted anticancer agents. *Nat Rev Drug Discov.* 2006;5:649-659.
- [37] Otsuka H, Nagasaki Y, Kataoka K. PEGylated nanoparticles for biological and pharmaceutical applications. *Adv Drug Deliv Rev.* 2003;55:403-419.
- [38] Ivashkevich A, Redon CE, Nakamura AJ, Martin RF, Martin OA. Use of the c-H2AX assay to monitor DNA damage and repair in translational cancer research. *Cancer Lett.* 2012;327:123-133.
- [39] Chugh BP, Lerch JP, Yu LX, et al. Measurement of cerebral blood volume in mouse brain regions using micro-computed tomography. *Neuroimage.* 2009;47:1312-1318.
- [40] Almeida J, Chen A, Foster A, Drezek R. In vivo biodistribution of nanoparticles. *Nanomedicine (Lond).* 2011;6:815-835.
- [41] Li SD, Huang L. Pharmacokinetics and biodistribution of nanoparticles. *Mol Pharm.* 2008;5:496-504.

How to cite this article: Davidi ES, Dreifuss T, Motiei M, et al. Cisplatin-conjugated gold nanoparticles as a theranostic agent for head and neck cancer. *Head & Neck.* 2017;00:1–9. <https://doi.org/10.1002/hed.24935>